Target fabrication for the POLAR experiment on the Orion laser facility

C. Spindloe, D. Wyatt, D. Haddock, I. East, J.E. Cross, C.N. Danson, E. Falize, J.M. Foster, M. Koenig and G. Gregori

High Power Laser Science and Engineering / Volume 3 / 2015 / e8
DOI: 10.1017/hpl.2015.2, Published online: 09 March 2015

High Power Laser Science and Engineering, (2015), Vol. 3, e8, 6 pages.

doi:10.1017/hpl.2015.2

Target fabrication for the POLAR experiment on the Orion laser facility

C. Spindloe[1], D. Wyatt[1], D. Haddock[1], I. East[1], J.E. Cross[2], C.N. Danson[2,3], E. Falize[4], J.M. Foster[2,3], M. Koenig[5], and G. Gregori[2]

[1]*Target Fabrication Group, Central Laser Facility, Rutherford Appleton Laboratory, Harwell Science and Innovation Campus, Didcot OX11 0QX, UK*

[2]*Atomic and Laser Physics, Clarendon Laboratory, University of Oxford, OX1 3PU, UK*

[3]*AWE, Aldermaston, Reading RG7 4PR, UK*

[4]*CEA-DAM-DIF, F-91297 Arpajon, France*

[5]*Laboratoire pour l'Utilisation Des Laser Intense, UMR 7605 CNRS-CEA-Ecole Polytechnique-Université Paris VI, Palaiseau, France*

(Received 15 November 2014; accepted 12 January 2015)

Abstract

This article describes the fabrication of a suite of laser targets by the Target Fabrication group in the Central Laser Facility (CLF), STFC Rutherford Appleton Laboratory for the first academic-access experiment on the Orion laser facility (Hopps *et al.*, Appl. Opt. **52**, 3597–3601 (2013)) at Atomic Weapons Establishment (AWE). This experiment, part of the POLAR project (Falize *et al.*, Astrophys. Space Sci. **336**, 81–85 (2011); Busschaert *et al.*, New J. Phys. **15**, 035020 (2013)), studied conditions relevant to the radiation-hydrodynamic processes occurring in a remarkable class of astrophysical star systems known as magnetic cataclysmic variables. A large number of complex fabrication technologies and research and development activities were required to field a total of 80 high-specification targets. Target design and fabrication procedures are described and initial alignment and characterization data are discussed.

Keywords: astrophysics; microtargets

1. Introduction

The target-fabrication group within the Central Laser Facility (CLF) has extensive expertise in the areas of micro-assembly, thin-film coating, target characterization and micromachining. The group was established to support the academic user community having access to the lasers within the CLF. The Atomic Weapons Establishment (AWE) Orion laser–plasma interaction facility[1] became operational in 2013 and as part of its remit makes up to 15% of its operational time available for experiments by the UK academic community and their international collaborators. The CLF supports this access by providing laser targets for these experiments.

The POLAR project[2, 3] aims to replicate in the laboratory some of the hydrodynamic processes occurring in X-ray binary star systems known as magnetic cataclysmic variables[4, 5]. In these binary stars, matter from a cold star is gravitationally accelerated towards a dense, white-dwarf companion star. Collimation of this flow by the white-dwarf's intense magnetic field results in a so-called accretion column of material at the poles of the star, instead of the usual accretion disc. The flow of material towards the star is impeded by the white-dwarf atmosphere and a reverse shock wave that is established in this column, near the surface of the white dwarf. The exceptionally high temperatures generated by this shock wave result in X-ray emission, and so give rise to the classification X-ray binary star. The purpose of the Orion experiment was to build a laboratory analogue of this process, in which the hydrodynamic processes could be studied in a controlled manner. The experiment uses high-power laser pulses to generate high-velocity plasma flow (collimated not by a magnetic field as in the star, but by a miniature surrounding tube) which impacts on the surface of an obstacle that mimics the white dwarf, resulting in the reverse shock wave that the experiment aims to study. The experimental layout is shown in Figure 1.

The main interaction target was the POLAR target, designed to produce the high-temperature plasma conditions

Correspondence to: C. Spindloe, Science and Technology Facilities Council, Rutherford Appleton Laboratory, Harwell Oxford, Chilton, Didcot, Oxon OX11 0QX, UK. Email: chris.spindloe@scitechprecision.com

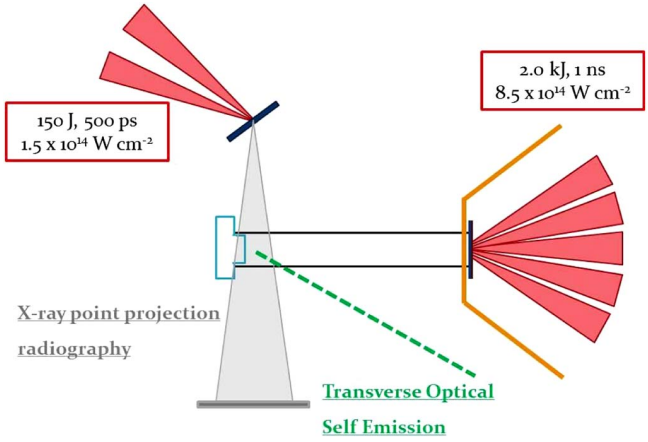

Figure 1. Experimental layout for the Orion POLAR campaign.

that were of interest to the experimental group. This is shown in Figure 1 as the horizontal tube which is 3.5 mm long and 550 μm internal diameter (650 μm outside diameter). Five nanosecond beams of the Orion laser are directed on to an ablator-pusher laser target, consisting of a multi-layered gold–plastic, or brominated plastic, foil with CH ablator, producing the plasma flow down the tube. The grey block at the end of the tube is the obstacle, made of quartz or steel. This target was mounted onto the Orion target positioner.

Secondary to this, a backlighter target was required to provide an X-ray image of the target during the interaction[6, 7]. This target is shown at the top of Figure 1, where two of the Orion beamlines are used to generate plasma whose X-ray emission was the backlighting source. The resulting X-ray image was recorded on the other side of the POLAR target using X-ray imaging plates. This backlighting target was positioned on a separate target mount designed to be inserted from a Ten Inch Manipulator (TIM), a diagnostic-insertion device mounted in the Orion target chamber.

The targets utilized the full scope of the target-fabrication group's capabilities and also required research and development into new, cost-effective materials.

2. POLAR interaction target

2.1. Specification

The POLAR interaction target was a combination of:

(1) a polyimide (PI) tube inside which the material could flow, and which was used to mimic the magnetic collimation that occurs in the binary star system;

(2) a quartz or steel obstacle, against which the material flow stagnates to generate the required reverse shock wave;

(3) a low-density foam sample;

(4) a washer for holding the target material;

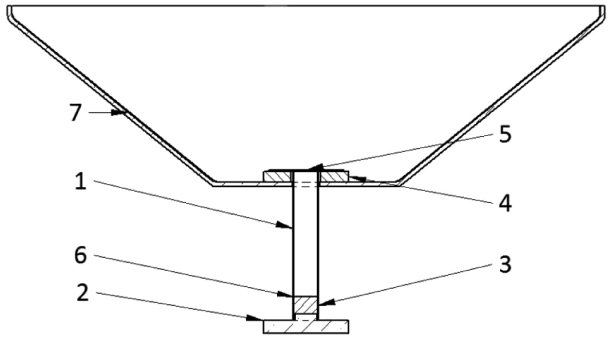

Figure 2. A CAD representation of the target sliced through the centreline (annotations are described in the text above).

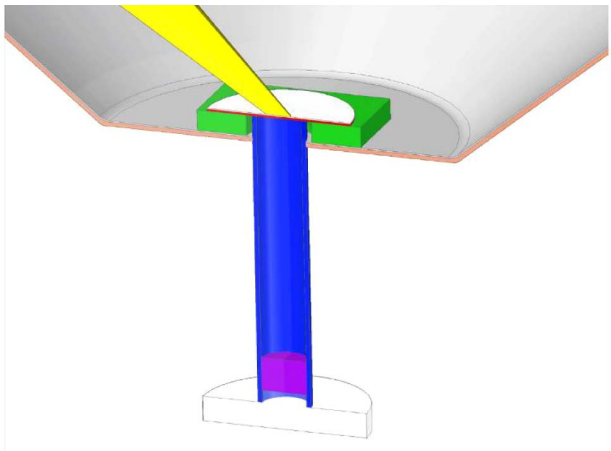

Figure 3. Shows a 3D CAD cut away of the target and indicates the positions of the pusher foil position and also shows the foam insert at the bottom of the tube.

(5) a pusher material that was either a brominated plastic, a gold/plastic multi-layer assembly, or a chlorinated plastic;

(6) a slit in the wall of the tube to allow a diagnostic view of the flow and of the shock wave whose X-ray emission was recorded by the AWE 'Dante'[8] diagnostic, and

(7) a copper cone to shield the diagnostics from scattered light from the incident laser beams.

These numbers correspond to the features in Figure 2.

The detailed design of this target underwent a number of modifications during the campaign. A number of alignment features and coatings were added to protect the target and to allow for the positioning of the target in the Orion chamber. These included small-diameter copper wires placed transversely across the tube as fiducial reference points to measure the propagation of the shock, and fibres on the target stalk to provide reference points for very precise alignment in the Orion target chamber. A 3D representation is shown

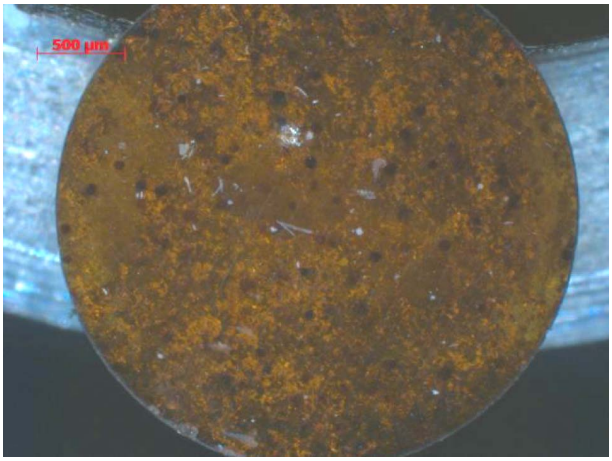

Figure 4. A fully processed Brominated plastic disk showing internal structure (dark areas are the un-melted material).

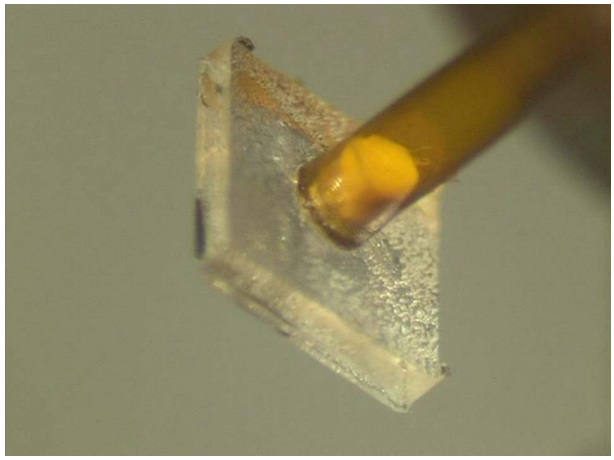

Figure 5. A low-density sample placed at the end of the PI tube next to the quartz obstacle.

in Figure 3, depicting just one of the five laser beams, shown in yellow, incident onto the pusher foils.

2.2. Brominated foil

Brominated plastic for the pusher material was not commercially available in the thickness required and purchasing a bespoke made foil was not possible within the budget. A research programme was initiated to press plastic films of brominated plastic from a commercially available powder. A heated press was used that had previously been used to manufacture deuterated plastic films. A number of tests were carried out to heat and mould bromopolystryene (C_8H_7Br) that had a bromine content of 43% by weight.

Initial results of pressing CHBr had mixed success, and temperature, pressure and mass were all important variables in producing a good quality film. At low temperatures (<200 °C) the powder did not show significant melt and was just fused together to form a brittle pressed pellet that was too thick. When the temperature was increased to ∼280 °C the sample showed signs of melt and the use of the correct amount of material produced a film ∼25 µm thick. However it can be seen in Figure 4 that the sample has not undergone a full melt as there are features of the order of 50 µm that are visible as dark areas in the disk and these correspond to the initial particle size of the powder used to manufacture the films.

To produce more uniform films a temperature of >300 °C would be required. Initial scanning electron microscope (SEM) analysis using energy-dispersive X-ray spectroscopy (EDX) confirms that there is bromine content still present after processing although there is some structure that is present in the pressed disk that is due to the target foil not going through a full melt when forming as shown in Figure 4.

Further characterization work using oxygen flask combustion, followed by ion chromatography has shown that the bromine levels of the samples analysed by mass percent was 31.10 (m/m%)[9] in correlation with the initial brominated powder that was 43% by weight. There is some loss of Bromine that is seen that requires further investigation.

2.3. Foam insert

Low-density foam of density 300 mg/cm^3 was to be placed at the end of the PI tube. The foam was required to be positioned next to the obstacle and was required to be 400 µm in length. The foam was manufactured using a critical point drying (CPD) technique[10] and a number of techniques were trialled to form the foam inside the tube. Firstly to make the foam *in situ* the PI tube was filled with the production liquid and UV cured. However filling of the liquid in the tube was not reproducible and therefore the foam did not cure to the correct length. The foam was then manufactured in a PMMA tube which transmits UV; however when running the CPD process the tube is incompatible with the chemicals and therefore lost shape and the foam produced was contaminated and distorted. The solution was to manufacture the foam in a tube that would survive the process (PI) and was UV transmissive. The foam was then removed from the tube, cut to length and re-inserted inside the final assembly tube. An example of the foam *in situ* can be seen in Figure 5.

2.4. Final target assembly

The remaining target components were produced using precision micromachining (washer and cone shield) and thin-film coating techniques (gold–plastic multi-layered pusher), and were integrated into the final target assembly as shown in Figure 6. The target is mounted on an AWE Orion mount with a cross brace to stabilize the cone. There

Figure 6. Images of the POLAR target from the obstacle side (left) the Au/CH pusher (right).

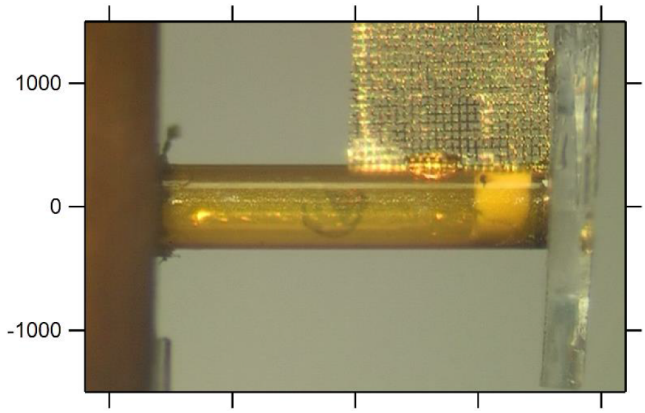

Figure 7. A side view of the foam inside the tube with the grid above.

is a 400 lines/inch (63 μm spacing) gold grid for spatial calibration of the X-ray backlighting images, as shown in Figure 7. The Dante diagnostic slit, although not visible, has been laser machined into the wall of the tube.

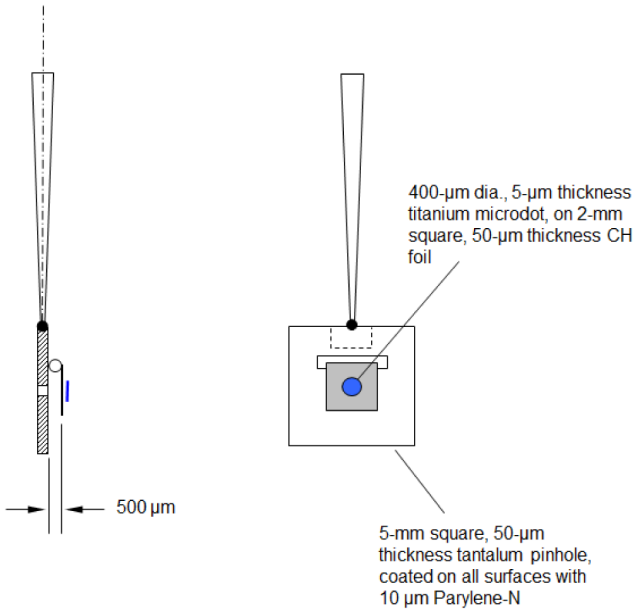

Figure 8. The backlighter target design.

3. Backlighter target

The backlighter target assembly design is shown in Figure 8. The X-ray backlighting source was the helium-like resonance line radiation from laser targets of chlorine (Parylene D), scandium, and titanium (respectively 2.79, 4.32 and 4.75 keV X-ray energy), chosen to highlight different features of the hydrodynamic flow in the X-ray absorption images. These different backlighter materials were cut into 400 μm diameter dots using laser machining and glued onto a CH support that was purchased commercially. This was then placed 500 μm from a tantalum pinhole that had been coated with 10 μm of Parylene-N (to prevent hydrodynamic closure of the tantalum pinhole, following X-ray ablation by the nearby backlighting plasma). This assembly was then attached to an Orion target mount, as shown in Figure 9, for positioning in the Orion target chamber.

4. X-ray target imaging

Sample backlighter images are shown in Figure 10. The Orion laser parameters together with the target design used to produce these images are detailed in Table 1. These images are produced from targets that are laser driven, but with a very short delay on the drive beams of only 4.75 ns. As such, no plasma has yet reached the end of the tube and they can

Table 1. Details of the Orion laser and POLAR target parameters for the images in Figure 10.

Image	Main target type	Drive beams total energy (kJ)	BL beams total energy (J)	BL beams pulse length (ns)	Delay between cones (ns)	Filters on SPCA	Filters on image plate	Step wedge
10(a)	CHBr Dante slit and grid	2.1	710	1	4.75	10 μm Ti + 2 ×50 μm plastic	8 μm aluminized mylar	50 μm, 100 μm, 150 μm C_2H_6
10(b)	CHBr foam and Al flash on quartz	2.4	780	1	4.75	10 μm Ti + 2 ×50 μm plastic	8 μm aluminized mylar	N/A

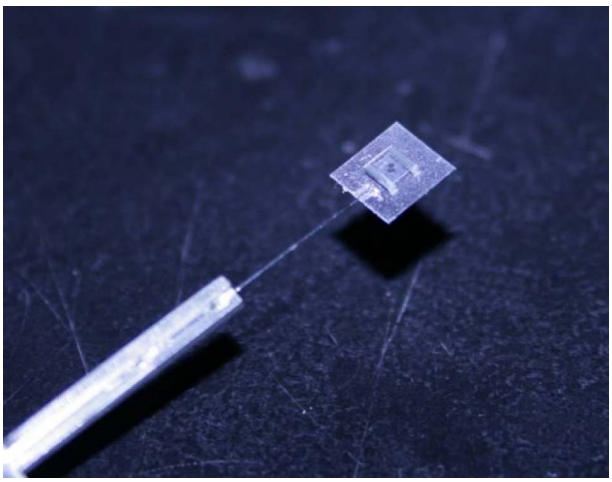

Figure 9. The fully assembled backlighter target.

therefore be used to distinguish the target features described earlier. The two images used in Figure 10 were produced on two independent shots with two different targets. In Figure 10(a) the target features the gold calibration grid (shown optically in Figure 7) and Dante slits in the PI tube; whilst in Figure 10(b) the target is seen with the foam in side the PI tube. The clearly defined grid structure evident in Figure 10(a) gives a resolution of the backlighting image of ∼10 μm.

5. Conclusions

A total of 80 targets (34 POLAR and 46 backlighter) were delivered for two periods of two weeks of academic access on Orion during November 2013 and February 2014. The development of a number of new target-fabrication techniques at the CLF, Rutherford Appleton Laboratory has enhanced the capabilities that are available and has contributed to a successful academic-access campaign. Further work is to be carried out to enhance the quality of the brominated plastic pushers to remove defect points in the target that may lead to instabilities in the plasma as it propagates down the tube and also to produce more uniform foam next to the obstacle.

References

1. N. Hopps, C. Danson, S. Duffield, D. Egan, S. Elsmere, M. Girling, E. Harvey, D. Hillier, M. Norman, S. Parker, P. Treadwell, D. Winter, and T. Bett, Appl. Opt. **52**, 3597 (2013).
2. E. Falize, B. Loupias, A. Ravasio, C. D. Gregory, A. Diziere, M. Koenig, C. Michaut, C. Cavet, P. Barroso, J.-P. Leidinger, X. Ribeyre, J. Breil, H. Takabe, Y. Sakawa, Y. Kuramitsu, T. Morita, N. C. Woolsey, W. Nazarov, and S. Pikuz, Astrophys. Space Sci. **336**, 81 (2011).
3. C. Busschaert, E. Falize, B. Loupias, C. Michaut, A. Ravasio, A. Pelka, R. Yurchak, and M. Koenig, New J. Phys. **15**, 035020 (2013).

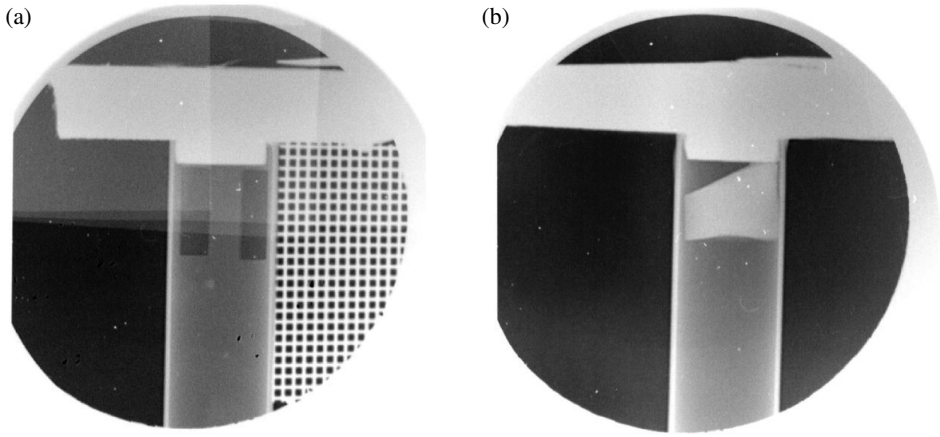

Figure 10. Sample backlighter images showing: (a) the PI tube with the quartz/steel obstacle at the top, the diagnostic slits cut in to the tube and the gold resolution grid attached to the target and (b) the PI tube with the quartz/steel obstacle at the top and a low-density foam insert below the stop.

4. D. Ryutov, R. P. Drake, J. Kane, E. Liang, B. A. Remington, and W. M. Wood-Vasey, Astrophys. J. **518**, 821 (1999).
5. E. Falize, C. Michaut, and S. Bouquet, Astrophys. J. **730**, 96 (2011).
6. R. R. Whitlock, S. P. Obenschain, and J. Grun, Appl. Phys. Lett. **41**, 429 (1982).
7. C. C. Kurantz, B. E. Blue, R. P. Drake, H. F. Robey, J. F. Hansen, J. P. Knauer, M. J. Grosskopf, C. Krauland, and D. C. Marion, Rev. Sci. Instrum. **77**, 10E327 (2006).
8. C. D. Bently, R. D. Edwards, J. E. Andrew, S. F. James, M. D. Gardner, A. J. Comley, K. Vaughan, C. J. Horsfield, M. S. Rubery, S. D. Rothman, S. Daykin, S. J. Masoero, J. B. Palmer, A. L. Meadowcroft, B. M. Williams, E. T. Gumbrell, J. D. Fyrth, C. R. D. Brown, M. P. Hill, K. Oades, M. J. Wright, B. A. Hood, and P. Kemshall, Rev. Sci. Instrum. **83**, 10D732 (2012).
9. Analysis report from Loughborough Surface Analysis Ltd (Oct 2014).
10. J. W. Falconer, W. Nazarov, and C. J. Horsfield, J. Vac. Sci. Technol. A **13**, 1941 (1995).